The EMBO Journal (2007) 26, 867–877 | © 2007 European Molecular Biology Organization | All Rights Reserved 0261-4189/07
www.embojournal.org

THE EMBO JOURNAL

Structural conservation of RecF and Rad50: implications for DNA recognition and RecF function

Olga Koroleva[1], Nodar Makharashvili[1], Charmain T Courcelle[2], Justin Courcelle[2] and Sergey Korolev[1,*]

[1]Edward A Doisy Department of Biochemistry and Molecular Biology, Saint Louis University School of Medicine, St Louis, MO, USA and [2]Department of Biology, Portland State University, Portland, OR, USA

RecF, together with RecO and RecR, belongs to a ubiquitous group of recombination mediators (RMs) that includes eukaryotic proteins such as Rad52 and BRCA2. RMs help maintain genome stability in the presence of DNA damage by loading RecA-like recombinases and displacing single-stranded DNA-binding proteins. Here, we present the crystal structure of RecF from *Deinococcus radiodurans*. RecF exhibits a high degree of structural similarity with the head domain of Rad50, but lacks its long coiled-coil region. The structural homology between RecF and Rad50 is extensive, encompassing the ATPase subdomain and the so-called 'Lobe II' subdomain of Rad50. The pronounced structural conservation between bacterial RecF and evolutionarily diverged eukaryotic Rad50 implies a conserved mechanism of DNA binding and recognition of the boundaries of double-stranded DNA regions. The RecF structure, mutagenesis of conserved motifs and ATP-dependent dimerization of RecF are discussed with respect to its role in promoting presynaptic complex formation at DNA damage sites.

The EMBO Journal (2007) **26,** 867–877. doi:10.1038/sj.emboj.7601537; Published online 25 January 2007
Subject Categories: structural biology
Keywords: DNA binding; Rad50; RecF; recombination; structure

Introduction

DNA damage encountered during replication can generate gaps in newly synthesized DNA, arrest progression of the replication machinery, or lead to breakdown of the replication fork and double-stranded (ds) DNA breaks (DSBs) (Cox *et al*, 2000). When these events are not accurately repaired, they can result in mutations, genomic rearrangements, or even cell lethality. Recombination proteins play essential roles in maintaining replication in the presence of DNA damage and allowing replication to resume (Kuzminov, 2001; Cox, 2002). In *Escherichia coli*, the homologous recombination proteins are classified into two predominant RecA-dependent pathways, the RecBCD pathway, and the RecF pathway (Kowalczykowski *et al*, 1994; Kuzminov, 1999). RecB, RecC and RecD function as a heterotrimeric complex that processes DSBs and is required for recombination during conjugation or transduction (Roman and Kowalczykowski, 1989). Interestingly, the recombination and repair defects in *recBC* mutants are efficiently suppressed by mutations in *sbcA*, *sbcB*, or *sbcCD* as long as the RecF pathway is functional (Bidnenko *et al*, 1999).

RecF, RecO, and RecR proteins form an epistatic group important for repair of single-stranded (ss) DNA gaps (SSGs) such as when replication is prematurely disrupted (Horii and Clark, 1973; Wang and Smith, 1984; Kolodner *et al*, 1985; Asai and Kogoma, 1994; Courcelle *et al*, 1997; Courcelle and Hanawalt, 2003). Homologs of RecFOR genes are found more frequently within bacterial genomes than are homologs of RecBCD (Rocha *et al*, 2005). For example, RecBC homologs are absent in the extremely DNA damage-resistant bacteria *Deinococcus radiodurans*, whereas homologs of RecFOR are present (Makarova *et al*, 2001). Several eukaryotic proteins such as WRN, BLM, RAD52, and BRCA2 share homology or functional similarities to RecF pathway genes, and are associated with a predisposition to cancer and aging when mutated (Karow *et al*, 2000; Mohaghegh and Hickson, 2001; Kowalczykowski, 2005; Yang *et al*, 2005).

The RecFOR proteins are thought to act by promoting the formation of RecA nucleoprotein filaments on ssDNA, also called presynaptic complexes, by overcoming the inhibitory function of ssDNA-binding protein (SSB) (Brent and Ptashne, 1980; Kolodner *et al*, 1985; Sassanfar and Roberts, 1990; Umezu *et al*, 1993; Cox *et al*, 2000; Courcelle *et al*, 2001; Courcelle and Hanawalt, 2003; Morimatsu and Kowalczykowski, 2003). The DNA-bound RecA filament is important for rec-dependent repair and serves as a sensor that signals the upregulation of the cellular 'SOS' genes in response to DNA damage. This function places RecF, -O and -R in a ubiquitous family of recombinational mediators (RMs) that are found in all organisms (Beernink and Morrical, 1999; Kowalczykowski, 2005). The mechanism by which RMs facilitate loading of RecA-like recombinases on SSB or RPA protected ssDNA is not understood.

Among RecF, -O, and -R, RecO is the least conserved. It possesses a DNA strand annealing activity that is similar to that of eukaryotic Rad52 (Luisi-DeLuca and Kolodner, 1994; Kantake *et al*, 2002; Makharashvili *et al*, 2004). Both proteins can anneal ssDNA coated by cognate ssDNA-binding proteins, suggesting specific protein–protein interactions between RecO and SSB. The crystal structure of RecO suggests potential sites of interaction with other proteins and DNA (Makharashvili *et al*, 2004; Leiros *et al*, 2005). RecR, the most

*Corresponding author. Department of Biochemistry and Molecular Biology, St Louis University School of Medicine, 1402 South Grand Blvd, St Louis, MO 63104, USA. Tel.: +1 314 977 9261; Fax: +1 314 977 9205; E-mail: korolevs@slu.edu

Received: 10 July 2006; accepted: 8 December 2006; published online: 25 January 2007

conserved of the three proteins, can interact with either RecO or RecF and has been proposed to functionally tether these proteins together, potentially mediating the sequential steps required for presynaptic complex formation to occur (Umezu and Kolodner, 1994; Webb *et al*, 1997; Bork *et al*, 2001; Morimatsu and Kowalczykowski, 2003). Together, RecO and RecR can promote RecA nucleation on SSB-coated ssDNA (Umezu *et al*, 1993; Shan *et al*, 1997; Bork *et al*, 2001). The crystal structure of RecR in *D. radiodurans* revealed a tetrameric clamp that could encircle dsDNA (Lee *et al*, 2004). The tetrameric clamp structure is also conserved in crystals of RecR from *Haemophilus influenza* (data in preparation). A DNA clamp may serve as an important component that tethers RM complexes to sites of DNA damage. The observation that RecR does not bind DNA by itself under physiological conditions (Webb *et al*, 1995) suggests that an as-yet unknown clamp-loading activity may be required in the RM reaction.

Addition of RecF to *in vitro* reactions was shown to be required for efficient presynaptic complex formation to occur specifically at ss/dsDNA junctions when only a substoichiometric amounts of RecFOR were present relative to SSB and RecA, even under conditions with the excess of SSB (Morimatsu and Kowalczykowski, 2003). This finding confirmed earlier hypothesis that RecF may properly position RecOR on specific DNA sites to initiate presynaptic complex formation (Sandler and Clark, 1994). Interestingly, the efficient loading of the eukaryotic Rad51 recombinase on RPA-coated DNA by the BRCA2 homolog Brh2 was observed to occur at the identical ds/ssDNA junction substrates (Yang *et al*, 2005). The specific mechanisms by which RecF recognizes gapped DNA substrates, or coordinates interactions with RecO and -R proteins, are not known.

RecF, together with RecR, also prevents RecA filaments from extending beyond SSGs (Hegde *et al*, 1996; Webb *et al*, 1997). In *E. coli*, RecR interacts with RecF only when the latter is bound to DNA (Webb *et al*, 1999). The separate location of RecF, -O, and -R on chromosome (Rocha *et al*, 2005) and some genetic studies suggested that RecF may have multiple functions, independent of RecO or RecR (Rangarajan *et al*, 2002; Kidane *et al*, 2004). *In vitro*, RecF binds RecX, thus diminishing the negative regulatory effect of RecX during presynaptic complex formation (Drees *et al*, 2004; Lusetti *et al*, 2006). The detailed tertiary structure of RecF would be very instrumental to delineate various RecF activities and particularly to study mechanism of the presynaptic complex formation.

The amino-acid sequence of RecF contains three conserved motifs characteristic of ATP-binding cassette (ABC) ATPases: Walker A, Walker B, and a 'signature' motif. The ABC ATPases comprise a diverse family of proteins whose functions range from membrane transporters to DNA-binding proteins (review in Hopfner and Tainer, 2003). The latter includes DNA mismatch and nucleotide excision repair enzymes (Ban and Yang, 1998; Obmolova *et al*, 2000; Junop *et al*, 2001), structural maintenance of chromosome (SMC) proteins like cohesin and condensin (Strunnikov, 1998), and the DSB repair enzyme Rad50 (Hirano *et al*, 1995). SMCs and Rad50 are characterized by the presence of a long coiled-coil structural domain inserted between N- and C-terminal halves of the globular head domain (Haering *et al*, 2002). The ABC-type ATPases exhibit ATP-dependent dimerization, in which the signature motif residues interact with ATP bound to the opposite molecule (in *trans*) (Junop *et al*, 2001; Smith *et al*, 2002; Hopfner and Tainer, 2003; Moncalian *et al*, 2004). RecF lacks a coiled–coil region, but it does exhibit an ATP-dependent DNA binding and a slow DNA-dependent ATP hydrolysis activity, similar to other SMC-like proteins (Madiraju and Clark, 1992; Webb *et al*, 1995; Hegde *et al*, 1996). The SMC-like properties of RecF and their role in recombination mediation reaction have not been extensively characterized. However, a previous study demonstrated that the conserved lysine residue of the ATP-binding motif (Walker A) is critical for RecF function, an observation that would be consistent with the idea that ATP hydrolysis is involved (Sandler *et al*, 1992; Webb *et al*, 1999).

In this report, we describe the high-resolution structure of RecF from *D. radiodurans*. We present evidence that the three SMC conserved motifs are important for RecF function *in vivo*, and demonstrate that ATP binding triggers RecF dimerization. The RecF structure is highly homologous to the head domain of Rad50, including α-helices from which the long coiled-coil domain of Rad50 originates, implying a conserved mechanism of DNA binding and recognition of the boundaries of dsDNA regions by both proteins. The structural conservation to Rad50 permits us to model the probable mechanism for binding ds/ssDNA junction by the RecF dimer. Based on the SMC-like dimerization of RecF and together with previously reported ATP- and DNA-dependent interactions with RecR, we propose that RecF dimerization on DNA may serve to place an RecR tetramer clamp on DNA.

Results

RecF structure

RecF was crystallized in a monoclinic space group with one molecule in an asymmetric unit. The structure was solved at a resolution 1.62 Å using native and selenomethionine protein derivative crystals. The final *R*-factor and free-*R* were 16.3 and 21.2%, with excellent geometry (Supplementary Table S1). The RecF structure is composed of two domains (Figure 1A). The ATPase domain 1 is formed by two β-sheets wrapped around a central α-helix A and is similar to the Lobe I subdomain of the Rad50 head domain (Figure 1B and C). The first antiparallel β-sheet is formed by six N-terminal β-strands (2↓ 1↑ 4↓ 5↑ 6↓ 7↑). The β3 and β8 form parts of the second β-sheet, which is otherwise composed of the C-terminal β-strands (15↓ 14↑ 3↑ 13↑ 12↑ 8↑). These two β-layers form an almost continuous β-sheet with a small gap between β2 and β15. Domain 2 is mostly α-helical and is similar to the Lobe II subdomain of the Rad50 head domain. The three α-helices, αB, αG, and αH, form a layer on top of the C-terminal β-sheet of the first domain. The helices αC, αD, and an antiparallel 3-stranded β-sheet (9↑ 10↓ 11↑), with insertion of two short helices αE and αF, form the remainder of the second domain. In Rad50, helices corresponding to αC and αD extend into a long coiled-coil region, which is absent in RecF. The nucleotide-binding Walker A motif (P-loop) is at the N-terminus of αA, whereas the Walker B motif is at the C-terminus of β12 and the signature ABC motif resides in the second domain at the beginning of αG.

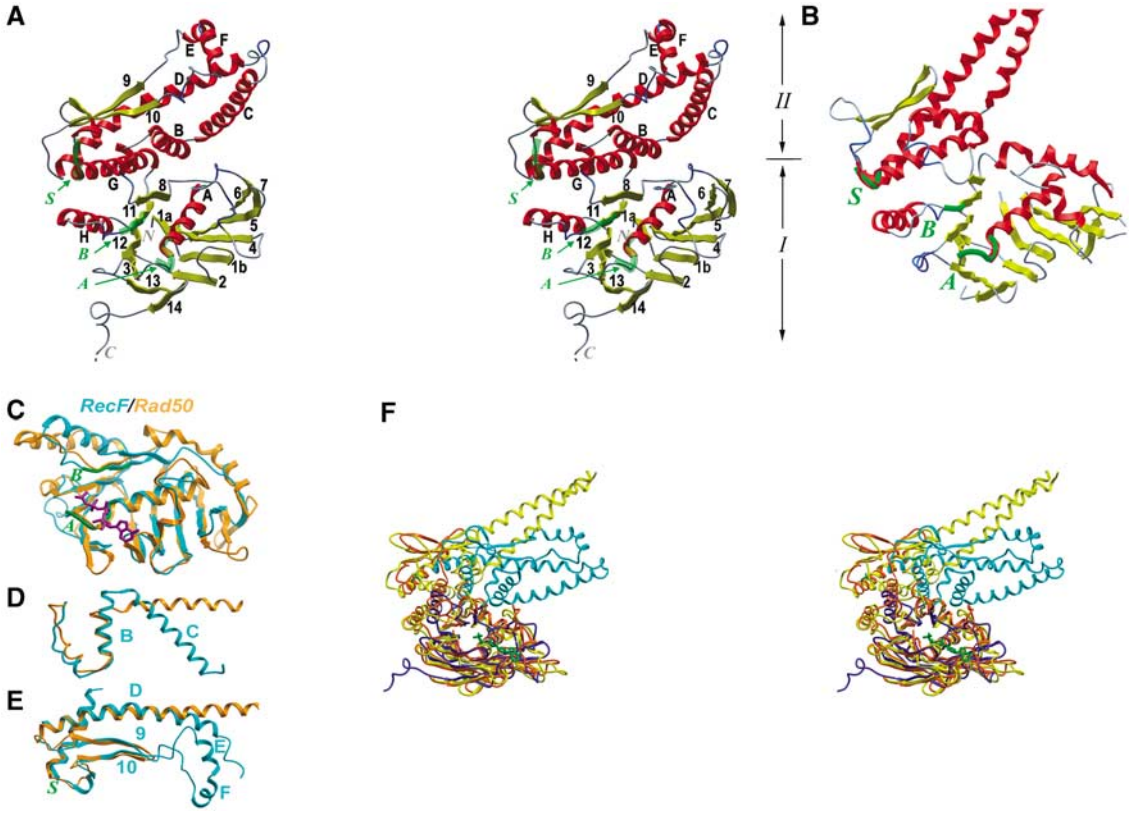

Figure 1 The structure of RecF is similar to the head domain of Rad50. (**A**) A ribbon representation of RecF in stereo view is shown. β-strands are numbered and shown in yellow and α-helixes are lettered and shown in red. Walker A, B, and signature motifs are highlighted in green and designated by letters A, B, and S correspondingly. Domains I and II are identified on the right. (**B**) A ribbon representation of the Rad50 (1ii8) structure with same color-coding of secondary structure elements. (**C**) A ribbon representation of the superimposed ATPase subdomains for RecF (cyan) and Rad50 (orange). (**D, E**) Superposition of Lobe II subdomains of RecF (cyan) and Lobe II of Rad50 (orange). The superposition was performed by overlaying the whole subdomains, but presented in two separate parts for clarity. Structural superposition and figures in the paper were performed with the program ICM (http://www.molsoft.com)(Cardozo *et al*, 1995). (**F**) Stereoview of the superposition of RecF with two different conformations of Rad50 head domain. The Lobe I domain of RecF is shown in dark blue and Lobe II in cyan. Two conformations of the Rad50 head domains are shown: the conformation found in monomeric structure (1ii8) is shown in yellow, whereas conformation of head domain from the dimeric structure (1f2u) is shown in red. The structures were superimposed by ATPase subdomains. ATPγS molecule bound to Rad50 are shown in green stick representation.

Structural similarity with Rad50

Almost all structural elements found in RecF are present in Rad50, suggesting that there is a strong evolutionary connection between these proteins. The ATPase domain and the three α-helices above the second β-sheet (αB, αG, and αH) are common to all ABC-type ATPases. The helix αA and the surrounding β-strands of RecF superimpose with their structural counterparts of Rad50 with a root mean square deviation (r.m.s.d.) of 2.7 Å for 107 Cα atoms (Figure 1C). The structural elements surrounding the Walker A motifs of each protein have almost identical conformations. In contrast, β4–β7 on the opposite side of domain 1 forms a more compact structure in RecF than that of Rad50. RecF also lacks short α-helixes inserted instead of β7 and β8.

Surprisingly, the second domain of RecF, which is more diverse among ABC ATPases, shares an even higher degree of similarity to Rad50 than the ATP-binding domain. Essentially every α-helix and β-strand of Rad50's Lobe II subdomain is also present in RecF (Figure 1D, and E). Ninety-three Cα atoms of this domain are superimposed with their equivalent part in Rad50 with an r.m.s.d. of 2.2 Å. Likewise, in another SMC protein (PDB id: 1w1w (Haering *et al*, 2004)), 118 Cα atoms of this same region superimpose with an r.m.s.d. of 2.6 Å. Although the long coiled-coil inserts, characteristic of Rad50 and SMC proteins, are absent in RecF, the RecF's αC and αD helices overlap with the helices of Rad50 that extend into the coiled–coil domain. The only structural addition in this domain, which is unique to RecF, is the extension of the loop between β9 and β10 with two short α-helices (αE and αF).

The orientation of the subdomains relative to each other is slightly different between the two proteins (Figure 1F). In RecF, Lobe II is rotated around the Lobe I away from position of Lobe II in Rad50. As a result, the distance between the conserved serine in signature motif of RecF and Rad50 is 18 Å when the structures are superimposed by Walker A and B motifs. The different orientation of Lobe II subdomain in RecF may be a result of the more compact structure of Lobe I subdomain lacking two α-helixes (αB and αC in Rad50) at the C-terminal end of αA. Interestingly, this alignment moves the αH of Lobe I domain together with the Lobe II domain. The direction of this rotation is almost perpendicular to the direction of the Lobe II domain rotation that is observed in Rad50 upon ATP-dependent dimerization (Figure 1F).

Structure-based sequence alignment

Based on structural superposition, we derived a proper sequence alignment between Rad50 and RecF (Figure 2).

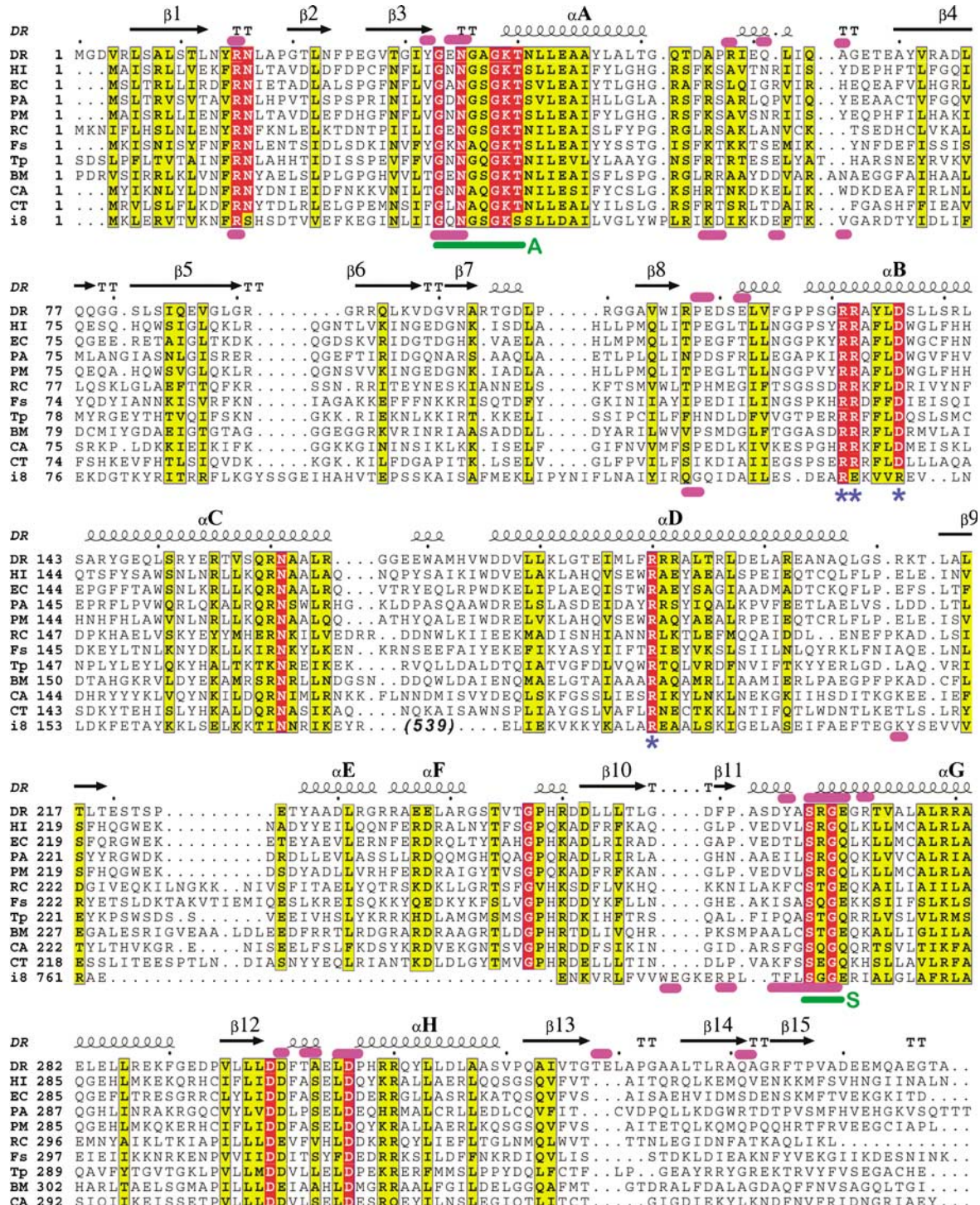

Figure 2 Multiple sequence alignment of 11 RecF proteins and *P. furiosus* Rad50. Sequence alignment was performed using the ClustalW program and plotted with the ESPript program (Thompson *et al*, 1994; Gouet *et al*, 1999). Similar residues as identified by the default ESPript parameters (Risler, global score 0.7) are highlighted in yellow, identical residues are in red. Alignment of Rad50 head domain sequence (i8 in diagram) is based on the structural alignment of RecF and pfRad50, with Rad50 residues highlighted in yellow and red if they are similar or identical to RecF consensus. Secondary structure elements of RecF are shown above the sequences. Conserved motifs are identified by green bars under the sequences with the letters A, B, S, and D for Walker A, B, signature and D-loop motifs. Magenta bars show residues involved in the predicted RecF dimerization (above sequences) and the known dimeric crystal structure of Rad50 (PDB ID: 1f2u) (below sequence). Residues that make up the partially buried charged cluster in Lobe II are identified by blue asterisks under the sequence. Abbreviations for organisms are as follows: DR, *D. radiodurans*; HI, *H. influenza*; EC, *E. coli*; PA, *P. aeruginosa*; PM, *P. multocida*; RC, *R. conorii*; Fs, *F. nucleatum*; Tp, *T. pallidum*; BM, *B. melitensis*; CA, *C. acetobutylicum*; CT, *C. trachomatis*; i8, *P. furiousus* Rad50.

Remarkably, most of the conserved residues in both domains of the bacterial RecF protein are also well preserved in Rad50, including the Walker A, Walker B, signature motifs, D-loop, and other residues. The only exception is the Q-loop, but in this case, a structurally similar loop is preserved in RecF.

A number of additional residues are also conserved between bacterial RecF and eukaryotic Rad50. The R15 between β1 and β2 is involved in the dimerization, nucleotide binding, and interacts with the potential DNA binding regions. The N35 of the P-loop is an essential part of the dimerization interface and is conserved only between RecF and Rad50 proteins (Figure 2; Hopfner *et al*, 2000), but not in the P-loops of other ABC ATPases.

Several polar residues in Lobe II of both proteins are fully or partially buried, surrounding the conserved R190 (Figures 2 and 4D). These residues include R131 (R153), R132 (E154), D136 (R158) of αB (αD), and R190 (R741) of αD (αE), where the corresponding residues and secondary structural elements of Rad50 are shown in parentheses. The preservation of these residues in such an unusual conformation across species and protein families strongly implies that they are important for protein function, possibly allosteric regulation.

Functional role of SMC conserved motifs

To address the role of the conserved motifs in RecF function, site-specific mutations were introduced into *E.coli* RecF to see if they could functionally complement an *E. coli recF* mutant. Two independent mutations were introduced into the Walker A motif (K36R and K36M; note that the *E. coli* sequence numbering is used, and not *D. radiodurans*). The K36R mutation prevents ATP hydrolysis, but not nucleotide binding. This mutation has been introduced previously in *E. coli* and is shown to be critical for RecF function (Sandler *et al*, 1992; Webb *et al*, 1999). A methionine at position 36 in place of lysine (K36M) has been shown in other Walker A motifs to prevent ATP binding. In the Walker B motif, we changed the aspartic acid at position 303 to an asparagine (D303N). In other SMC proteins, this change traps ATP in its transition state and stabilizes dimerization of the homodimer (Smith *et al*, 2002). Finally, in the signature motif, we substituted the serine at position 270 to arginine (S270R). In Rad50, the equivalent mutation interferes with ATP-dependent dimerization (Moncalian *et al*, 2004). The mutations were introduced in the *E. coli recF* in the pQE-9 vector. This *RecF* expression plasmid complemented the UV hypersensitivity of a *recF* mutant, even when expression was not induced by IPTG (Figure 3B), consistent with previous studies that found a low level of RecF expression was sufficient for function *in vivo* (Sandler and Clark, 1993). Each of the four RecF mutations failed to complement the UV hypersensitivity of the *recF* mutant, indicating that all three major SMC motifs in RecF are important for its role in UV resistance and supporting the idea that the roles of these conserved motifs are likely to be similar to their counterparts in other SMC proteins.

DNA-dependent ATPase activity of RecF

We observed a DNA-dependent ATPase activity of *D. radiodurans* RecF (Figure 3A) similar to that seen for the *E. coli* RecF (Webb *et al*, 1999). The rate of ATP hydrolysis was twofold higher in the presence of dsDNA ($0.22\,min^{-1}$) than with ssDNA ($0.1\,min^{-1}$). In the presence of the ss/dsDNA junction, the rate was $0.13\,min^{-1}$ and no ATPase activity was observed without DNA. Importantly, the signature motif mutation (S268R) prevented ATP hydrolysis, similar to that of Walker B D300N mutation (Figure 3A).

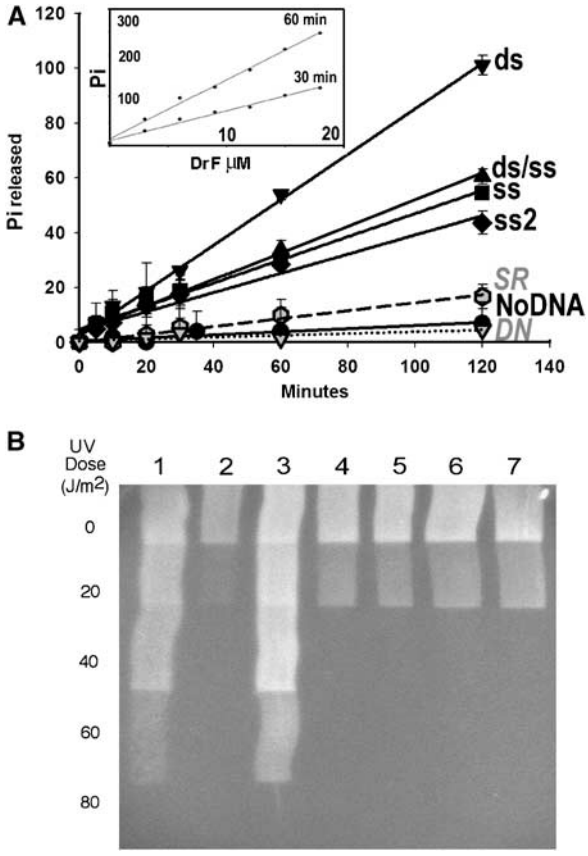

Figure 3 (**A**) *D. radiodurans* RecF is a DNA-dependent ATPase. The phosphate release over time by wild type (solid lines) RecF in the absence (black circles) and presence of DNA substrates: ss (black squares)—30-nt long ssDNA (TAT CCG CAG AGT TGG CTG GTA GTT CAG CCC); ss2 (black diamonds)—15-mer ssDNA (TAT CCG CAG AGT TGG); ds (black inverted triangles)—30-mer ssDNA annealed with a 30-mer complimentary strand; ds/ss (black triangles)—30-mer ssDNA annealed with a 15-mer complimentary strand (15-mer dsDNA with a 15-mer 3′ ssDNA tail). DNA concentration is 17 μM. ATPase activity of RecF mutants in the presence of 30-mer dsDNA is shown by dashed line with gray filled circles for S268R (signature motif) mutant, and by dotted line with gray filled triangles for D300N (Walker B motif) mutant. Lack of ATPase activity by lysine to arginine substitution in Walker A motif was previously reported (Webb *et al*, 1999). The insert diagram represents the phosphate release dependence on RecF concentration at 30 and 60 min in the presence of dsDNA. (**B**) Cells expressing RecF proteins mutated in the Walker A, B, or signature motif fail to complement a *recF* mutant in *E. coli* UV resistance assay. The survival of wild type (lane 1), *recF* vector (2), *recF* expressing the normal RecF protein (3), and *recF* expressing the site-specific RecF mutations K36R (4), K36M (5), S270R (6), or D303N (7) are shown following exposure to the indicated dose of UV irradiation (note the numbering of residues accordingly to the *E. coli* sequence).

The ATP-dependent dimerization of RecF

The ATP-dependent protein dimerization is a key step in regulating the function of all ABC ATPases that have been characterized to date (for a review, see Hopfner and Tainer, 2003). However, as most ABC ATPases are function as part of larger heterooligomeric complexes, it has been difficult to precisely identify when and what role the dimerization has in

a complex multistep reactions. In case of RecF, the dimerization could be important for DNA binding, recognition of ss/dsDNA junction, interactions with other protein partners, such as RecR, or for a combination of these events. As a first step towards dissecting this question, we examined whether RecF oligomerization occurred in the presence of ATP.

Initial attempts to utilize the size-exclusion chromatography (SEC) alone were complicated owing to the tendency of RecF to aggregate and due to potential nonspecific interactions of RecF with gel-filtration matrices resulted in late elution of RecF comparatively to standard protein markers (Supplementary Figure S1). Delay of RecF elution varied depending on different buffers, presence of nucleotide, and gel-filtration matrices. Therefore, the molecular weight (MW) of the eluted protein species was directly measured by the subsequent multiangle static light scattering analysis (SLS) (Supplementary Figure S1). Under most conditions, including the presence of 2 mM ATP in a low-salt (0.1 M KCl) running buffer, the SLS measurements resulted in a MW of $38 \pm 10\%$ kDa, corresponding to a monomer. Only when highly concentrated protein was loaded (2 mg/ml and higher) on the column, equilibrated with 2 mM ATP in low salt, the SLS estimated MW was $78 \pm 10\%$ kDa, even though the elution volume of the dimer was closer to those of 44 kDa marker (BioRad). Thus, RecF forms an ATP-induced dimer even in the absence of DNA, although requirement for high concentration pointed to relatively low dimerization constant. These data also explained previously reported apparent monomeric state of *E. coli* RecF in the presence of 1mM ATP as estimated by gel filtration method only (Webb *et al*, 1999).

We also addressed the role of SMC conserved motifs in ATP-dependent dimerization of RecF. Because of complications connected with the protein solubility and dimer stability during gel filtration, we utilized the dynamic light scattering (DLS) method, which allows direct measurements of hydrodynamic radius (R_h) of the complexes in solution under equilibrium conditions, as opposed to the SEC method. The observed R_h are shown in Table I. Under conditions that the SEC/SLS analysis demonstrated only the presence of the monomer (no ATP or high salt 1 M KCl), the R_h of RecF was determined to be in a range of 3.4–3.7 nm. In an ideal sphere approximation, it corresponds to an apparent MW of 60–68 kDa, and the difference with the expected MW of RecF of 40 kDa can be explained by the elongated shape of the globule. Under conditions favorable for the dimer formation (see above), the R_h was between 4.2–4.5 nm, corresponding to the almost doubled apparent MW of 100–115 kDa. The standard deviations (polydispersity) of all reported DLS measurements were less than 15%, indicating monodisperse distributions. The differences between mean values were in 2–4% range under similar protein concentration conditions. Interestingly, the stable dimer was observed only with RecF concentrations above 0.2 mg/ml (5 μM) at 20°C, pointing to the low dimerization constant in a micromolar range. It is possible, that other interactions with DNA or RecR can farther stabilize RecF dimer.

The Walker A motif mutant K39R, which supposedly binds, but does not hydrolyze ATP, also forms dimers under similar to the wild-type RecF dimerization conditions. The dimerization was not observed with the wild type protein in the presence of ADP even under high protein concentration. The Walker A motif mutant K39M, which does not bind ATP, did not form dimers. Finally, mutation of the signature motif, which is predicted to interact with ATP only in a dimeric state, disrupted the ability of RecF to dimerize, even under high protein concentration. Thus, DLS experiments further supported the ATP-dependent dimerization of RecF mediated by the signature motif similarly to the dimerization of Rad50.

Table I DLS measurements

	Prot. conc. (mg/ml)	KCl conc. (M)	Nucleotide	R_h (nm)	Polydisp (%)
WT	0.8	0.1	ATP	4.5	13
WT	0.8	1.0	ATP	3.6	14
WT	1.1	0.1	ADP	3.7	10
WT	0.33	0.1	—	3.4	12
WT	0.4	0.1	ATP	4.2	16
K39R	0.5	0.1	ATP	4.2	13
K39M	0.6	0.1	ATP	3.4	15
S267R	1.4	0.1	ATP	3.6	16

The R_h and the polydispersity values are an average of at least three separate measurement cycles. Differences between the observed R_h deviated by less than 5% between cycles.

Modeling of RecF dimerization

The requirement for the signature motif to interact with the γ-phosphate group of nucleotide bound in trans during dimerization allowed us to model the structure of the RecF dimer with reasonable certainty (Figure 4). The model was accomplished by superimposing the ATPase domains of two RecF molecules with those of the Rad50 dimer bound to ATPγS (Hopfner *et al*, 2000). To compensate for the rotational differences between the Lobe II subdomains of Rad50 and RecF, the placement of one RecF monomer was adjusted to minimize the distance between conserved serine of the signature motif of each monomer and the γ-phosphate groups of nucleotides modeled into the Walker A motif. The resulting RecF dimer formed a semi-clamp or symmetrical crab-claw that has two arms extending in the directions similar to those of coiled–coil regions of Rad50 dimer (Hopfner *et al*, 2001). The claw structure contains sufficient space to accommodate and cradle dsDNA bound within the pocket region. It is important to note that modeling of the dimer was based entirely on conformation of the conserved motifs, and that no special adjustments were performed to optimize the shape of the predicted DNA-binding surface.

The surface area of the monomer that becomes buried upon dimerization was 1200 Å^2, as calculated with the CNS program (Brunger *et al*, 1998), 15% smaller than that observed in the Rad50 dimer (1400 Å^2). It is noteworthy that in this model, the majority of conserved residues map to the dimerization interface and pocket region of the claw, where DNA binding is expected to occur (Figure 4D). This conservation is preserved through Rad50 as well (Figure 2). Additionally, although the overall surface of RecF is predominantly negatively charged, the inside surface of the dimer cradle is more positively charged, favoring DNA binding (Figure 4B, upper panel).

Discussion

The high-resolution structure of RecF presented here reveals extensive similarity with the head domains of SMC proteins

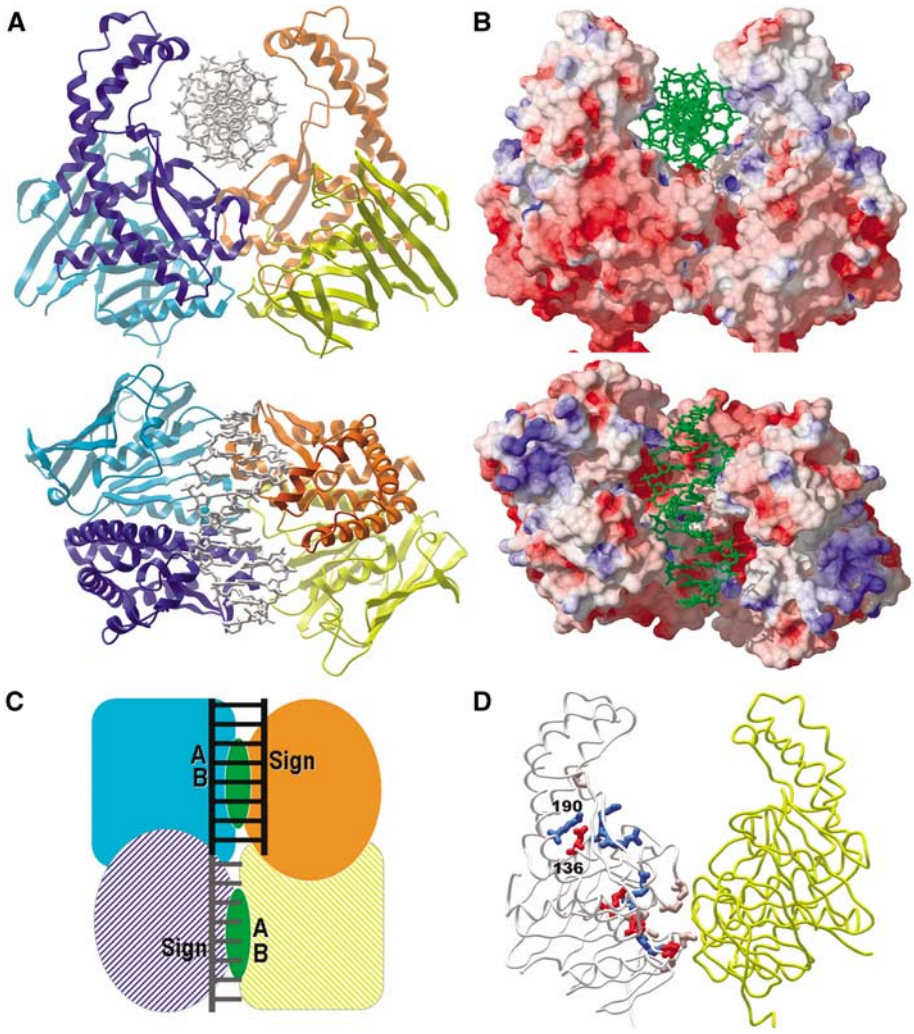

Figure 4 Model of RecF dimer and DNA binding. (**A**) A ribbon representation of potential RecF dimer with Lobe I and II of one monomer colored in yellow and orange respectively, and those of the second monomer in cyan and dark blue. The bottom panel is the view from the top of the orientation shown in upper panel. The B-form dsDNA is shown as gray sticks. (**B**) Surface representation of RecF dimer color-coded according to the surface electrostatic potential, calculated with REBEL (Rapid Exact-Boundary Electrostatics) method as implemented in the ICM program with maximum color potential set at ± 5 kT/e (Totrov and Abagyan, 1996; Totrov and Abagyan, 2001). Molecules are shown in the same orientations as in (A). DNA is shown in green. (**C**) The proposed model of asymmetric DNA binding to RecF dimer. ATPase domains are shown as rectangles and Lobe II domains as ovals with same color coding as in (A). ATP-binding sites are depicted as green ovals. DNA is schematically shown on the top in black and gray. Binding of dsDNA (black) in vicinity of one ATP-binding site and ssDNA (gray) to the other is speculated to have different effect on conformational changes and ATPase properties of each half of the dimer as depicted by different filing modes of each subunit. (**D**) The RecF dimer is shown in worm representation with conserved RecF residues of one monomer shown as sticks and color-coded accordingly to their polarity. Two residues of conserved polar residues buried in Lobe II subdomain are numbered.

and the DSB repair protein Rad50. This homology was not shared with other ABC ATPases involved in DNA repair, such as MutS (Obmolova *et al*, 2000; Junop *et al*, 2001). The structural similarities reflect protein function, as the repair activities of RecF pathway proteins are not directly involved in the removal of DNA lesions, but, similar to Rad50, promote DNA repair through recruitment of other recombination proteins.

Rad50 plays critical roles in DSB repair in archaea and eukaryotes. In *E. coli*, the predominant DSB repair pathway is RecBC, whereas RecF is classically thought to function in the repair of ssDNA gaps. However, the RecF pathway efficiently repairs DSBs in *E. coli* when either component of the SbcC/SbcD complex has been inactivated. Interestingly, SbcC is thought to be the *E. coli* ortholog of Rad50 because it possesses the SMC motifs, includes the long central coiled–coil domain, and forms complexes with the nuclease SbcD, similar to Rad50/Mre11 complex (Connelly *et al*, 1998; Connelly and Leach, 2002). The structural similarities presented here suggest a strong evolutionary connection between RecF, SbcC, and Rad50, and one can speculate that RecF and SbcC may compete for the same DNA substrates in *E. coli* under certain conditions.

The globular head domains play central roles in SMC and Rad50 proteins activities. However, it is difficult to asses biochemically how these structures function, owing to experimental obstacles of working with these large proteins that in addition to their extremely long coiled-coil inserts, also function as components of larger protein complexes. The high degree of structural conservation that extends across different protein families and between prokaryotes and eukaryotes strongly implies that the head domains of

Rad50, RecF, and SbcC share a common function in DNA metabolism. Therefore, studies with the globular RecF protein should prove helpful in dissecting the mechanism of activities of these structural domains.

In addition to overall structural similarities, we also demonstrated that all ABC motifs in RecF are important for UV resistance in *E. coli*. We showed that RecF forms dimers in the presence of ATP and that mutations within the signature motif prevent such dimerization. Thus, both structural and functional studies support the idea that RecF and the head domains of Rad50 share similar mechanistic properties. This functional similarity provides an opportunity to use the globular RecF protein as a model to gain further insights into mechanism of Rad50 DNA recognition.

The structure presented here points to the importance of the Lobe II subdomain in DNA recognition. Indeed, in spite of a generally weaker conservation of the Lobe II subdomain across all ABC-type ATPases, this subdomain is more structurally conserved between RecF and Rad50 than the ATPase Lobe I subdomain. The conformation of the signature motif in Lobe II is important for regulation of ATPase activity and dimer assembly in both Rad50 and RecF. In each case, the Lobe II subdomain is connected to the ATPase domain by flexible linkers, suggesting a common mechanism for allosteric regulation within the dimeric structures, where different factors, such as DNA and other protein partners, may affect the conformation of the Lobe II subdomain and, correspondingly, of the signature motif.

The presence of several conserved charged residues clustered around the fully buried R190 suggests an additional flexible region in Lobe II. By analogy, a cluster of buried charged resides is present in *E. coli* DNA polymerase I at the bottom of finger domains, where a large 30° rotation of the domain occurs during nucleotide incorporation (Korolev *et al*, 1995; Li *et al*, 1998). In Rad50, the charged cluster is at the base of the coiled–coil region, neighboring the predicted Mre11-binding site (Hopfner *et al*, 2001). Thus, structural flexibility in this region may be involved in allosteric regulation between the Mre11-binding site and signature motif conformation. In RecF, the long coiled-coil region is replaced by a small arm formed with αE and αF at the tip, which may wrap around dsDNA in the modeled dimeric structure. Although this region is less conserved than ATP-binding and dimerization surfaces, the analysis of RecF structure for potential protein interaction sites using the optimal docking areas program (ODA) predicted that this region is a potential protein–protein interaction site (Fernandez-Recio *et al*, 2005). Thus, this cluster of buried charged residues in RecF may be important for allosteric regulation between the signature motif conformation and interaction of the Lobe II domain with other protein partners.

An important question in the field of DSB repair is how Rad50 recognizes blunt-ended DNA (de Jager *et al*, 2001). RecF functions at a ds/ssDNA junction (Morimatsu and Kowalczykowski, 2003). Thus, the structural similarity between Rad50 and RecF suggests that both proteins may utilize similar mechanisms of dsDNA boundary recognition. One explanation may be derived from the models of dimer–DNA complexes proposed here (Figure 4) and previously (Hopfner *et al*, 2001). Both suggest that Rad50 and RecF dimers can bind extended (14–16 bp) dsDNA regions (Figure 4A). One-half of the bound DNA (7–8 bp) will interact with one ATP-binding site formed by the ATPase domain of monomer A and the Lobe II domain of monomer B, while the other half will bind around the second ATP molecule between ATPase domain of monomer B and the Lobe II domain of monomer A (Figure 4C). Consequently, interaction of the two ATP-binding sites with different DNA substrates (ssDNA versus dsDNA in case of RecF and dsDNA versus empty site in case of Rad50) may result in specific asymmetrical conformational changes within the dimer. In the case of RecF, we and others found that dsDNA stimulates ATPase hydrolysis at a higher rate than ssDNA (Figure 3A), an effect that likely reflects different conformations of ATP-binding sites bound to these substrates. We would suggest that such specific conformational states of the dimer would be more important for interaction of RecF and Rad50 with their protein partners, rather than for formation of a DNA binding surface with higher affinity for dsDNA end. In our preliminary studies of RecF interactions with oligonucleotides, we did not observe preferential binding to ss/dsDNA junctions as compared to dsDNA (data not shown) consistent with previous studies (Webb *et al*, 1999). Thus, the proposed conformational changes caused by asymmetric binding of two ATP sites to ds- and ssDNA fragments, may be important for regulating or activating RecF interactions with protein partners, such as RecR at the appropriate ss/dsDNA junction. Similarly, in Rad50, the asymmetric conformation of the dimer bound to blunt-ended DNA as described above may initiate the signaling cascade by Mre11–Rad50 complex (Lee and Paull, 2005). More quantitative studies of the interplay between the RecF ATP-dependant dimerization, DNA binding, ATP hydrolysis and RecF interactions with other protein partners are required to fully understand mechanism DNA damage recognition by RecF and Rad50 proteins.

An attractive possibility to consider for the role that RecF dimerization may have in recombination mediation reaction is also suggested by the crystal structure of RecR (Lee *et al*, 2004). RecR forms a tetrameric ring similar in shape to DNA clamp proteins. As both dimeric and tetrameric species of RecR from different organisms were previously observed in solution (Umezu and Kolodner, 1994; Lee *et al*, 2004), a dimer to tetramer transition has been proposed as a DNA loading mechanism. RecR interacts with RecF during presynaptic complex formation (Webb *et al*, 1995; Morimatsu and Kowalczykowski, 2003). In *E. coli*, RecR does not efficiently bind DNA or RecF under physiological conditions, but forms stable complexes with DNA-bound RecF in a manner that attenuates RecF-mediated ATP hydrolysis (Webb *et al*, 1995). Taken together, these observations suggest that the ATP-dependent dimerization of RecF on DNA may serve as a clamp loading mechanism that joins two RecR dimers to form a tetrameric clamp on the DNA. The recent finding that RecR from *Thermus thermophilus* binds RecF with 4:2 stoichiometry further supports this idea (Honda *et al*, 2006).

The surprisingly high degree of structural similarity between structures of RecF and Rad50 provides an opportunity to use comparative analysis to dissect the mechanism of DNA binding and allosteric regulation of these proteins and to explain their biochemical properties. Future structure-guided mutagenesis studies of the RecF DNA binding and protein interaction properties should provide further insight into the mechanism by which related recombination mediators act, in both prokaryotes and eukaryotes.

Materials and methods

Cloning, expression, purification, and crystallization

recF was amplified from *D. radiodurans* R1 genomic DNA (American Type Culture Collection), cloned into pMCSG7 as described (Stols *et al*, 2002), and expressed in the *E. coli* strain BL21(DE3) pLysS (Novagen). Cells were harvested by centrifugation, lysed in buffer containing 1.0 M NaCl, 20% glycerol, 0.5 M NDSB-201, 50 mM HEPES pH 7.5, 0.1% Triton-X 100, 5 mM βME, 1 mM PMSF, and 0.5 mg/ml lysozyme. Cells were sonicated and the insoluble cellular material was removed by centrifugation. The RecF was purified using Ni-NTA (Qiagen) affinity chromatography, incubated with TEV protease to cleave the N-terminal His-tag, and passed again through an NiNTA column to remove His-tagged proteins and other contaminants with elevated NiNTA affinity.

RecF was crystallized using a hanging drop vapor diffusion method in buffer containing 2.5 M $(NH_4)_2SO_4$, 20% sucrose, 0.1 M HEPES pH 8.0. Initially, only shapeless aggregates appeared after few days with heavy background precipitation, and were used for streak seeding procedure. The final crystals were monoclinic with cell dimensions $a = 47.9$ Å, $b = 87.4$ Å, $c = 52.9$ Å, $\beta = 115^\circ$, containing one molecule per asymmetric unit. Selenomethionine (SeMet) protein derivatives were obtained according to a previously described protocol (Walsh *et al*, 1999) and were crystallized by the same seeding technique using native protein crystals.

Data collection and structure determination

The crystals of native protein diffracted to a resolution of 1.6 Å and SeMet-substituted crystals to a 2.0 Å at 19ID SBC beam line, APS, ANL. The diffraction data were processed with HKL2000 (Otwinowski and Minor, 1997). The structure was solved using native and SeMet MAD data sets with the autoSHARP program, which automatically performed all steps from data scaling to the model building with the ARP/wARP program (Perrakis *et al*, 1999; Bricogne *et al*, 2003), resulting in building of about 85% of the structure. The model was completed and refined using native data with programs O and REFMAC (Jones *et al*, 1991; Murshudov *et al*, 1999). The data collection and refinement statistics are shown in Table I. The structure factors and coordinates have been deposited into PDB with accession code 2O5V.

RecF mutagenesis

Site-specific mutations were generated on the pMSCG7 plasmid using the Quick-change II site directed mutagenesis kit (Stratagene) and confirmed by sequencing. For UV resistance assays, the *recF* gene from *E. coli* was cloned into the *Bam*HI site of the expression vector pQE-9 (Qiagen), and mutations were introduced as described above.

UV resistance

The ability of each *recF* mutant plasmid to confer UV-resistance in *E. coli*, and therefore complement, *recF* mutants was then determined by irradiating *recF* cultures that contained each expression plasmid. Complementation of UV sensitivity was determined using fresh overnight cultures that were evenly applied to a Luria–Bertani medium plate using a cotton swab. The plate was covered by a sheet of aluminum foil and placed under a 15-W germicidal lamp (254 nm; 0.6 J/m^2/s). The foil was then progressively retracted following 20-J/m^2 exposures. The irradiated plate was then incubated at 37°C for 8 h and photographed.

ATPase activity

The ATPase activity of *D. radiodurans* RecF in the presence of different oligonucleotides was analyzed using malachite green assay (Bioassay systems). Proteins were purified as described above with the additional gel filtration step using Sephacryl-200 16/60 preparative column (GE Healthcare/Lifesciences). The final reaction mixture included 10% PEG 6K, 14% glycerol, 1% DMSO, 150 mM KCl, 20 mM HEPES pH 8.0, 10 mM $MgCl_2$, 0.5 mM TCEP, 2 mM ATP, and 17 μM of DNA oligonucleotides. Oligonucleotides were obtained from Integrated DNA Technologies. Reactions were initiated by the addition of RecF to the final concentration of 3.75 μM or as stated otherwise, and carried out at 20°C. The reaction was stopped by addition of HCl ($pH = 2$) at various time points, mixed with the malachite green reagent, and the optical density (OD) was measured on a plate reader after incubation at 20°C for 10 min (Molecular devices, Thermomax microplate reader, Softmax). Standard P_i curve was plotted according to the manufacturer's protocol. Standard errors of the measurements were calculated form three independent experiments.

RecF dimerization

To address oligomeric states of RecF in solution we utilized SEC in conjunction with multiangle SLS techniques using TSK-GEL G3000S analytical gel filtration column (Tosoh Bioscience) mounted on AKTA FPLC (GE Healthcare) and connected with miniDAWN SLS device (Wyatt Inc.). The MW of protein species eluted from the column was calculated with ASTRA V 5.1.6 software (Wyatt Inc).

The hydrodynamic radiuses (R_h) of the protein aggregates in solution were measured with the dynamic light scattering techniques (DLS) with DynaPro Titan instrument (Wyatt Inc) in batch mode. The protein was dialyzed over night against final buffer containing 10% glycerol, 20 mM HEPES pH 8.0, 5% DMSO, 1 mM TCEP, 0.1 or 1.0 M KCl, and 2 mM of nucleotide when stated. Dialyzed protein was cleared by centrifugation and subjected to filtering through 20-nm Anatop 10 filter (Whatman). The protein concentration was not adjusted to avoid protein aggregation caused by disturbance, because of high propensity of RecF to aggregate, and as even the fraction of a percent of high molecular weight aggregates can considerably reduce the accuracy of DLS measurements. The R_h was calculated based on statistic of 100 measurements of 5 s each. The final numbers were accepted only when three or more consecutive cycles resulted in a stable (within 5% difference) R_h and polydispersity measurements (Supplementary Figure S2). Solution viscosity was calculated with 'Sednterp' (Sedimentation Interpretation) program, v1.08 (Hayes DB, Laue T, Philo J), and tested with BSA.

Supplementary data

Supplementary data are available at *The EMBO Journal* Online (http://www.embojournal.org).

Acknowledgements

These works were supported by the EA Doisy Trust Fund and SLU Medical School Start Up Fund and by NIH grant GM073837. JC, CTC are supported by National Science Foundation Career Award MCB0551798. We are grateful to the staff of SBC at beam line 19ID for providing beam time. Use of the Argonne National Laboratory Structural Biology Center beamlines at the Advanced Photon Source was supported by the US Department of Energy, Office of Biological and Environmental Research, under Contract No. W-31-109-ENG-38.

References

Asai T, Kogoma T (1994) The RecF pathway of homologous recombination can mediate the initiation of DNA damage-inducible replication of the *Escherichia coli* chromosome. *J Bacteriol* **176:** 7113–7114

Ban C, Yang W (1998) Crystal structure and ATPase activity of MutL: implications for DNA repair and mutagenesis. *Cell* **95:** 541–552

Beernink HT, Morrical SW (1999) RMPs: recombination/replication mediator proteins. *Trends Biochem Sci* **24:** 385–389

Bidnenko V, Seigneur M, Penel-Colin M, Bouton MF, Dusko Ehrlich S, Michel B (1999) sbcB sbcC null mutations allow RecF-mediated repair of arrested replication forks in rep recBC mutants. *Mol Microbiol* **33:** 846–857

Bork JM, Cox MM, Inman RB (2001) The RecOR proteins modulate RecA protein function at 5' ends of single-stranded DNA. *EMBO J* **20:** 7313–7322

Brent R, Ptashne M (1980) The lexA gene product represses its own promoter. *Proc Natl Acad Sci USA* **77:** 1932–1936

Bricogne G, Vonrhein C, Flensburg C, Schiltz M, Paciorek W (2003) Generation, representation and flow of phase information in structure determination: recent developments in and around SHARP 2.0. *Acta Crystallogr D* **59:** 2023–2030

Brunger AT, Adams PD, Clore GM, DeLano WL, Gros P, Grosse-Kunstleve RW, Jiang JS, Kuszewski J, Nilges M, Pannu NS, Read RJ, Rice LM, Simonson T, Warren GL (1998) Crystallography & NMR system: a new software suite for macromolecular structure determination. *Acta Crystallogr D* **54:** 905–921

Cardozo T, Totrov M, Abagyan R (1995) Homology modeling by the ICM method. *Proteins* **23:** 403–414

Connelly JC, Kirkham LA, Leach DR (1998) The SbcCD nuclease of *Escherichia coli* is a structural maintenance of chromosomes (SMC) family protein that cleaves hairpin DNA. *Proc Natl Acad Sci USA* **95:** 7969–7974

Connelly JC, Leach DR (2002) Tethering on the brink: the evolutionarily conserved Mre11–Rad50 complex. *Trends Biochem Sci* **27:** 410–418

Courcelle J, Carswell-Crumpton C, Hanawalt PC (1997) recF and recR are required for the resumption of replication at DNA replication forks in *Escherichia coli*. *Proc Natl Acad Sci USA* **94:** 3714–3719

Courcelle J, Hanawalt PC (2003) RecA-dependent recovery of arrested DNA replication forks. *Annu Rev Genet* **37:** 611–646

Courcelle J, Khodursky A, Peter B, Brown PO, Hanawalt PC (2001) Comparative gene expression profiles following UV exposure in wild-type and SOS-deficient *Escherichia coli*. *Genetics* **158:** 41–64

Cox MM (2002) The nonmutagenic repair of broken replication forks via recombination. *Mutat Res* **510:** 107–120

Cox MM, Goodman MF, Kreuzer KN, Sherratt DJ, Sandler SJ, Marians KJ (2000) The importance of repairing stalled replication forks. *Nature* **404:** 37–41

de Jager M, van Noort J, van Gent DC, Dekker C, Kanaar R, Wyman C (2001) Human Rad50/Mre11 is a flexible complex that can tether DNA ends. *Mol Cell* **8:** 1129–1135

Drees JC, Lusetti SL, Cox MM (2004) Inhibition of RecA protein by the *Escherichia coli* RecX protein: modulation by the RecA C terminus and filament functional state. *J Biol Chem* **279:** 52991–52997

Fernandez-Recio J, Totrov M, Skorodumov C, Abagyan R (2005) Optimal docking area: a new method for predicting protein-protein interaction sites. *Proteins* **58:** 134–143

Gouet P, Courcelle E, Stuart DI, Metoz F (1999) ESPript: analysis of multiple sequence alignments in PostScript. *Bioinformatics* **15:** 305–308

Haering CH, Lowe J, Hochwagen A, Nasmyth K (2002) Molecular architecture of SMC proteins and the yeast cohesin complex. *Mol Cell* **9:** 773–788

Haering CH, Schoffnegger D, Nishino T, Helmhart W, Nasmyth K, Lowe J (2004) Structure and stability of cohesin's Smc1-kleisin interaction. *Mol Cell* **15:** 951–964

Hegde SP, Rajagopalan M, Madiraju MV (1996) Preferential binding of *Escherichia coli* RecF protein to gapped DNA in the presence of adenosine (gamma-thio) triphosphate. *J Bacteriol* **178:** 184–190

Hirano T, Mitchison TJ, Swedlow JR (1995) The SMC family: from chromosome condensation to dosage compensation. *Curr Opin Cell Biol* **7:** 329–336

Honda M, Inoue J, Yoshimasu M, Ito Y, Shibata T, Mikawa T (2006) Identification of the RecR toprim domain as the binding site for both RecF and RecO: A role of RecR in RecFOR assembly at dsDNA-ssDNA junctions. *J Biol Chem* **281:** 18549–18559

Hopfner KP, Karcher A, Craig L, Woo TT, Carney JP, Tainer JA (2001) Structural biochemistry and interaction architecture of the DNA double-strand break repair Mre11 nuclease and Rad50-ATPase. *Cell* **105:** 473–485

Hopfner KP, Karcher A, Shin DS, Craig L, Arthur LM, Carney JP, Tainer JA (2000) Structural biology of Rad50 ATPase: ATP-driven conformational control in DNA double-strand break repair and the ABC-ATPase superfamily. *Cell* **101:** 789–800

Hopfner KP, Tainer JA (2003) Rad50/SMC proteins and ABC transporters: unifying concepts from high-resolution structures. *Curr Opin Struct Biol* **13:** 249–255

Horii Z, Clark AJ (1973) Genetic analysis of the recF pathway to genetic recombination in *Escherichia coli* K12: isolation and characterization of mutants. *J Mol Biol* **80:** 327–344

Jones TA, Zou JY, Cowan SW, Kjeldgaard M (1991) Improved methods for binding protein models in electron density maps and the location of errors in these models. *Acta Crystallogr A* **47:** 110–119

Junop MS, Obmolova G, Rausch K, Hsieh P, Yang W (2001) Composite active site of an ABC ATPase: MutS uses ATP to verify mismatch recognition and authorize DNA repair. *Mol Cell* **7:** 1–12

Kantake N, Madiraju MV, Sugiyama T, Kowalczykowski SC (2002) *Escherichia coli* RecO protein anneals ssDNA complexed with its cognate ssDNA-binding protein: A common step in genetic recombination. *Proc Natl Acad Sci USA* **99:** 15327–15332

Karow JK, Wu L, Hickson ID (2000) RecQ family helicases: roles in cancer and aging. *Curr Opin Genet Dev* **10:** 32–38

Kidane D, Sanchez H, Alonso JC, Graumann PL (2004) Visualization of DNA double-strand break repair in live bacteria reveals dynamic recruitment of *Bacillus subtilis* RecF, RecO and RecN proteins to distinct sites on the nucleoids. *Mol Microbiol* **52:** 1627–1639

Kolodner R, Fishel RA, Howard M (1985) Genetic recombination of bacterial plasmid DNA: effect of RecF pathway mutations on plasmid recombination in *Escherichia coli*. *J Bacteriol* **163:** 1060–1066

Korolev S, Nayal M, Barnes WM, Di Cera E, Waksman G (1995) Crystal structure of the large fragment of *Thermus aquaticus* DNA polymerase I at 2.5-Å resolution: structural basis for thermostability. *Proc Natl Acad Sci USA* **92:** 9264–9268

Kowalczykowski SC (2005) Cancer: catalyst of a catalyst. *Nature* **433:** 591–592

Kowalczykowski SC, Dixon DA, Eggleston AK, Lauder SD, Rehrauer WM (1994) Biochemistry of homologous recombination in *Escherichia coli*. *Microbiol Rev* **58:** 401–465

Kuzminov A (1999) Recombinational repair of DNA damage in *Escherichia coli* and bacteriophage lambda. *Microbiol Mol Biol Rev* **63:** 751–813

Kuzminov A (2001) DNA replication meets genetic exchange: chromosomal damage and its repair by homologous recombination. *Proc Natl Acad Sci USA* **98:** 8461–8468

Lee BI, Kim KH, Park SJ, Eom SH, Song HK, Suh SW (2004) Ring-shaped architecture of RecR: implications for its role in homologous recombinational DNA repair. *EMBO J* **23:** 2029–2038

Lee JH, Paull TT (2005) ATM activation by DNA double-strand breaks through the Mre11–Rad50–Nbs1 complex. *Science* **308:** 551–554

Leiros I, Timmins J, Hall DR, McSweeney S (2005) Crystal structure and DNA-binding analysis of RecO from *Deinococcus radiodurans*. *EMBO J* **24:** 906–918

Li Y, Korolev S, Waksman G (1998) Crystal structures of open and closed forms of binary and ternary complexes of the large fragment of *Thermus aquaticus* DNA polymerase I: structural basis for nucleotide incorporation. *EMBO J* **17:** 7514–7525

Luisi-DeLuca C, Kolodner R (1994) Purification and characterization of the *Escherichia coli* RecO protein. Renaturation of complementary single-stranded DNA molecules catalyzed by the RecO protein. *J Mol Biol* **236:** 124–138

Lusetti SL, Hobbs MD, Stohl EA, Chitteni-Pattu S, Inman RB, Seifert HS, Cox MM (2006) The RecF protein antagonizes RecX function via direct interaction. *Mol Cell* **21:** 41–50

Madiraju MV, Clark AJ (1992) Evidence for ATP binding and double-stranded DNA binding by *Escherichia coli* RecF protein. *J Bacteriol* **174:** 7705–7710

Makarova KS, Aravind L, Wolf YI, Tatusov RL, Minton KW, Koonin EV, Daly MJ (2001) Genome of the extremely radiation-resistant bacterium *Deinococcus radiodurans* viewed from the perspective of comparative genomics. *Microbiol Mol Biol Rev* **65:** 44–79

Makharashvili N, Koroleva O, Bera S, Grandgenett DP, Korolev S (2004) A novel structure of DNA repair protein RecO from *Deinococcus radiodurans*. *Structure (Cambridge)* **12:** 1881–1889

Mohaghegh P, Hickson ID (2001) DNA helicase deficiencies associated with cancer predisposition and premature ageing disorders. *Hum Mol Genet* **10:** 741–746

Moncalian G, Lengsfeld B, Bhaskara V, Hopfner KP, Karcher A, Alden E, Tainer JA, Paull TT (2004) The rad50 signature motif: essential to ATP binding and biological function. *J Mol Biol* **335:** 937–951

Morimatsu K, Kowalczykowski SC (2003) RecFOR proteins load RecA protein onto gapped DNA to accelerate DNA strand exchange. A universal step of recombinational repair. *Mol Cell* **11:** 1337–1347

Murshudov GN, Vagin AA, Lebedev A, Wilson KS, Dodson EJ (1999) Efficient anisotropic refinement of macromolecular structures using FFT. *Acta Crystallogr D* **55** (Part 1)**:** 247–255

Obmolova G, Ban C, Hsieh P, Yang W (2000) Crystal structures of mismatch repair protein MutS and its complex with a substrate DNA. *Nature* **407:** 703–710

Otwinowski Z, Minor W (1997) Processing of X-Ray diffraction data collected in oscillation mode. *Methods Enzymol* **276:** 307–326

Perrakis A, Morris R, Lamzin VS (1999) Automated protein model building combined with iterative structure refinement. *Nat Struct Biol* **6:** 458–463

Rangarajan S, Woodgate R, Goodman MF (2002) Replication restart in UV-irradiated *Escherichia coli* involving pols II, III, V, PriA, RecA and RecFOR proteins. *Mol Microbiol* **43:** 617–628

Rocha EP, Cornet E, Michel B (2005) Comparative and evolutionary analysis of the bacterial homologous recombination systems. *PLoS Genet* **1:** e15

Roman LJ, Kowalczykowski SC (1989) Characterization of the helicase activity of the *Escherichia coli* RecBCD enzyme using a novel helicase assay. *Biochemistry* **28:** 2863–2873

Sandler SJ, Chackerian B, Li JT, Clark AJ (1992) Sequence and complementation analysis of recF genes from *Escherichia coli*, *Salmonella typhimurium*, *Pseudomonas putida* and *Bacillus subtilis*: evidence for an essential phosphate binding loop. *Nucleic Acids Res* **20:** 839–845

Sandler SJ, Clark AJ (1993) Use of high and low level overexpression plasmids to test mutant alleles of the recF gene of *Escherichia coli* K-12 for partial activity. *Genetics* **135:** 643–654

Sandler SJ, Clark AJ (1994) RecOR suppression of recF mutant phenotypes in *Escherichia coli* K-12. *J Bacteriol* **176:** 3661–3672

Sassanfar M, Roberts JW (1990) Nature of the SOS-inducing signal in *Escherichia coli*. The involvement of DNA replication. *J Mol Biol* **212:** 79–96

Shan Q, Bork JM, Webb BL, Inman RB, Cox MM (1997) RecA protein filaments: end-dependent dissociation from ssDNA and stabilization by RecO and RecR proteins. *J Mol Biol* **265:** 519–540

Smith PC, Karpowich N, Millen L, Moody JE, Rosen J, Thomas PJ, Hunt JF (2002) ATP binding to the motor domain from an ABC transporter drives formation of a nucleotide sandwich dimer. *Mol Cell* **10:** 139–149

Stols L, Gu M, Dieckman L, Raffen R, Collart FR, Donnelly MI (2002) A new vector for high-throughput, ligation-independent cloning encoding a tobacco etch virus protease cleavage site. *Protein Expr Purif* **25:** 8–15

Strunnikov AV (1998) SMC proteins and chromosome structure. *Trends Cell Biol* **8:** 454–459

Thompson JD, Higgins DG, Gibson TJ (1994) CLUSTAL W: improving the sensitivity of progressive multiple sequence alignment through sequence weighting, position-specific gap penalties and weight matrix choice. *Nucleic Acids Res* **22:** 4673–4680

Totrov M, Abagyan R (1996) The contour-buildup algorithm to calculate the analytical molecular surface. *J Struct Biol* **116:** 138–143

Totrov M, Abagyan R (2001) Rapid boundary element solvation electrostatics calculations in folding simulations: successful folding of a 23-residue peptide. *Biopolymers* **60:** 124–133

Umezu K, Chi NW, Kolodner RD (1993) Biochemical interaction of the *Escherichia coli* RecF, RecO, and RecR proteins with RecA protein and single-stranded DNA binding protein. *Proc Natl Acad Sci USA* **90:** 3875–3879

Umezu K, Kolodner RD (1994) Protein interactions in genetic recombination in *Escherichia coli*. Interactions involving RecO and RecR overcome the inhibition of RecA by single-stranded DNA-binding protein. *J Biol Chem* **269:** 30005–30013

Walsh MA, Dementieva I, Evans G, Sanishvili R, Joachimiak A (1999) Taking MAD to the extreme: ultrafast protein structure determination. *Acta Crystallogr D* **55:** 1168–1173

Wang TV, Smith KC (1984) recF-dependent and recF recB-independent DNA gap-filling repair processes transfer dimer-containing parental strands to daughter strands in *Escherichia coli* K-12 uvrB. *J Bacteriol* **158:** 727–729

Webb BL, Cox MM, Inman RB (1995) An interaction between the *Escherichia coli* RecF and RecR proteins dependent on ATP and double-stranded DNA. *J Biol Chem* **270:** 31397–31404

Webb BL, Cox MM, Inman RB (1997) Recombinational DNA repair: the RecF and RecR proteins limit the extension of RecA filaments beyond single-strand DNA gaps. *Cell* **91:** 347–356

Webb BL, Cox MM, Inman RB (1999) ATP hydrolysis and DNA binding by the *Escherichia coli* RecF protein. *J Biol Chem* **274:** 15367–15374

Yang H, Li Q, Fan J, Holloman WK, Pavletich NP (2005) The BRCA2 homologue Brh2 nucleates RAD51 filament formation at a dsDNA-ssDNA junction. *Nature* **433:** 653–657